VIBRATIONAL SPECTRUM AND ELECTRONIC STRUCTURE OF 11-VERTEX *NIDO*-TRICARBABORANE 7,8,9-$C_3B_8H_{12}$ AS COMPARED TO ISOSTRUCTURAL $[7,9\text{-}C_2B_9H_{12}]^-$ SPECIES

Cite this: *INEOS OPEN*, **2019**, *2 (3)*, 105–111
DOI: 10.32931/io1915a

Received 2 April 2019,
Accepted 30 May 2019

http://ineosopen.org

L. A. Leites,* R. R. Aysin, S. S. Bukalov,
E. G. Kononova, and D. S. Perekalin

Nesmeyanov Institute of Organoelement Compounds, Russian Academy of Sciences, ul. Vavilova 28, Moscow, 119991 Russia

Abstract

A comparative study of two isostructural 11-vertex *nido*-carbaboranes, namely, neutral molecule 7,8,9-$C_3B_8H_{12}$ **1** and anion $[7,9\text{-}C_2B_9H_{12}]^-$ **2** is performed using vibrational spectroscopy and Bader's AIM analysis. Raman and IR spectra of **1**, **2** and their μ-deuterated analogs are investigated experimentally and analyzed by means of normal coordinate analysis (NCA). Complicated patterns of the vibrational bands corresponding to BHB bridges in the region of ~1700–2150 cm^{-1} are interpreted as being due to the strong Fermi resonance. The results of topological analysis of an electron density distribution function shows that BH_b bonds in the BHB bridge are nearly as strong as intracage B–B bonds, being equal partners in formation of the cage bonding system. Elongation of the B10–B11 distance under the bridge is explained by the fact that there is no edge-localized two-center bond between these atoms. Introduction of the third carbon atom into an open face of the *nido* cage is found to strengthen the C–H and terminal B–H bonds, but does not influence the BHB bridge.

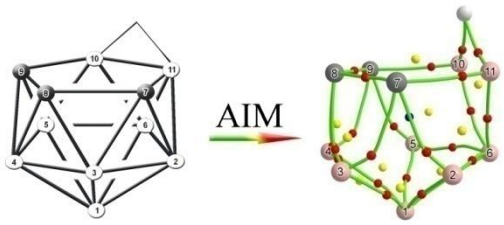

Key words: 11-vertex *nido*-carbaboranes, vibrational spectra, QTAIM analysis, electronic structure.

Introduction

Vibrational spectra of various polyhedral *closo* and *nido* carbaboranes have been widely investigated (the literature before 1992 is summarized in review [1]; for some subsequent papers, see Refs. [2–11]). However, all the species studied hitherto contained either one or two carbon atoms. Here we report the vibrational spectrum of a representative of carbaboranes containing three carbon atoms, namely, neutral molecule 7,8,9-$C_3B_8H_{12}$ **1**, first synthesized in 1995 [12] and belonging to a 11-vertex *nido*-carbaborane family (see Fig. 1 for a polyhedral framework with atom numbering). According to Ref. [13], this moderately stable substance does not form crystals suitable for X-ray crystallography. Only the MP2-optimized geometry is available for **1** [13, 14], which shows that molecule **1** is isostructural with $[7,9\text{-}C_2B_9H_{12}]^-$ anion **2**, known since the pioneering works of Hawthorne [15]. The X-ray structure of **2** was published in Refs. [16, 17], while the MP2 optimized geometries for **2** and for many of its methyl derivatives can be found elsewhere [18]. All the data show that the *"extra"* (or *"endo"* or *"acidic"* or *"facial"*) hydrogen atom forms a symmetric BHB bridge on the open face of these *nido* polyhedra, between atoms B10 and B11 (Fig. 1).

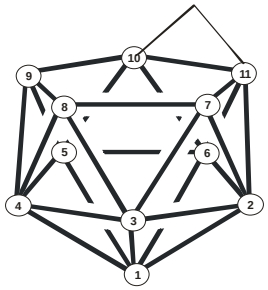

Figure 1. Traditional atom numbering of 11-vertex *nido*-polyhedron.

It seems reasonable to study experimentally and theoretically the hitherto unknown vibrational spectrum of **1** and its μ-*d*-substituted molecule **1d** in order to determine vibrational manifestations of the BHB bridge, to compare the data obtained with those for isostructural anion **2**, and to elucidate the influence of a carbon atom number on the spectral features. It is also of interest to investigate the electron bonding system in **1** and **2** by Bader's "Atoms in Molecules" (AIM) method [19], *i.e.*, to carry out the topological analysis of the electron density function. This approach has proven very useful for elucidating the details of electron-deficient borane and carbaborane structures [10, 11, 20–22].

In this paper, we report the full vibrational spectra of **1** and **2** (the latter as its Cs salt) and those of their μ-*d*-analogs as well as the results of DFT (B3LYP/6-311++G(d,p)) calculations of vibrational mode frequencies, intensities, and eigenvectors. QTAIM analysis of electron density distribution was performed at CCSD/cc-pVTZ level.

Results and discussion

1. Vibrational spectra

Only the IR data for **1** have been published in the Experimental Section of Ref. [13] as a set of figures. Some experimental data on the vibrational spectra for **2** and its derivatives have been given previously in papers [1, 23, 24] and in a Dr.Sci. thesis [25].

Here we report the Raman spectra of solid **1** and Cs salt of **2** as well as their μ-*d*-analogs in the region of 100–3700 cm^{-1} and also their IR spectra in the region of 200–4000 cm^{-1}. The results are presented in Table 1 and in Figs. 2–4 as well as Figs. S1 and S2 in Electronic supplementary information (ESI). Tables S1 and S2 in ESI also contain the calculated, unscaled harmonic frequencies and IR intensities of the normal modes along with their approximate description. The normal mode assignment to symmetry species and to particular molecular motions is based on the experimental data on Raman and IR activities, on depolarization ratios of the Raman lines, on comparison with the spectra of μ-deuterated species and on the results of normal coordinate analysis (NCA).

Isostructural species **1** and **2** differ only in the number of carbon atoms in their open faces. Both species **1** and **2** belong to the *C*s point symmetry group; their 63 normal modes are allocated to 35 A′ and 28 A″ symmetry species, both being active in Raman and IR spectra.

The spectrum of solid **1** exhibits a broad Rayleigh wing in the Raman region below 100 cm^{-1} (Fig. S2) and is characterized by rather broad bands without crystal splittings. These spectral peculiarities indicate that **1**, like neutral globular *closo*-carbaboranes [25, 26], forms a plastic mesophase at room temperature, in which the molecules, being fixed in sites of a crystal lattice by their centers of gravity, undergo rapid reorientations. Plasticity of **1**, also confirmed by easy sublimation of the compound, is the reason why **1** does not form crystals suitable for the X-ray analysis [13].

With an eye on the figures and tables, it is clear that the spectral patterns of **1** and **2** are very much alike and that the number of the spectral features observed is much less than the theoretical value (63). This fact can be easily explained in terms of the results of NCA, which show that the frequencies of normal modes, belonging to different symmetry species (A′ and A″) but having close eigenvectors, really coincide. It is natural

Table 1. Comparison of the frequencies of similar vibrations in the spectra of solid **1** and **2** and their μ-*d*-analogs[a]

Vibration type, symmetry species	**1**	μ-*d*-**1**	**2**	μ-*d*-**2**
νCH A′, A″	3070	3070	3031	3032
νBH_t	2597–2619	2595–2615	2520–2548	2510–2550
ν/δ BHB A′	calc. 1989	1430	calc. 1991	
	exp. 2110–1725		exp. 2120–1780	1470–1380
ν/δ BHB A″	calc. 1715	1381	calc. 1697	
δCH A′	1252	1250	1182	1181
Cage breathing A′	806	797	812	811
A″	791	774	767	772
Lowest frequency	498	498	463	462

[a] μ-*d* means deuteration of the *extra* hydrogen atom.

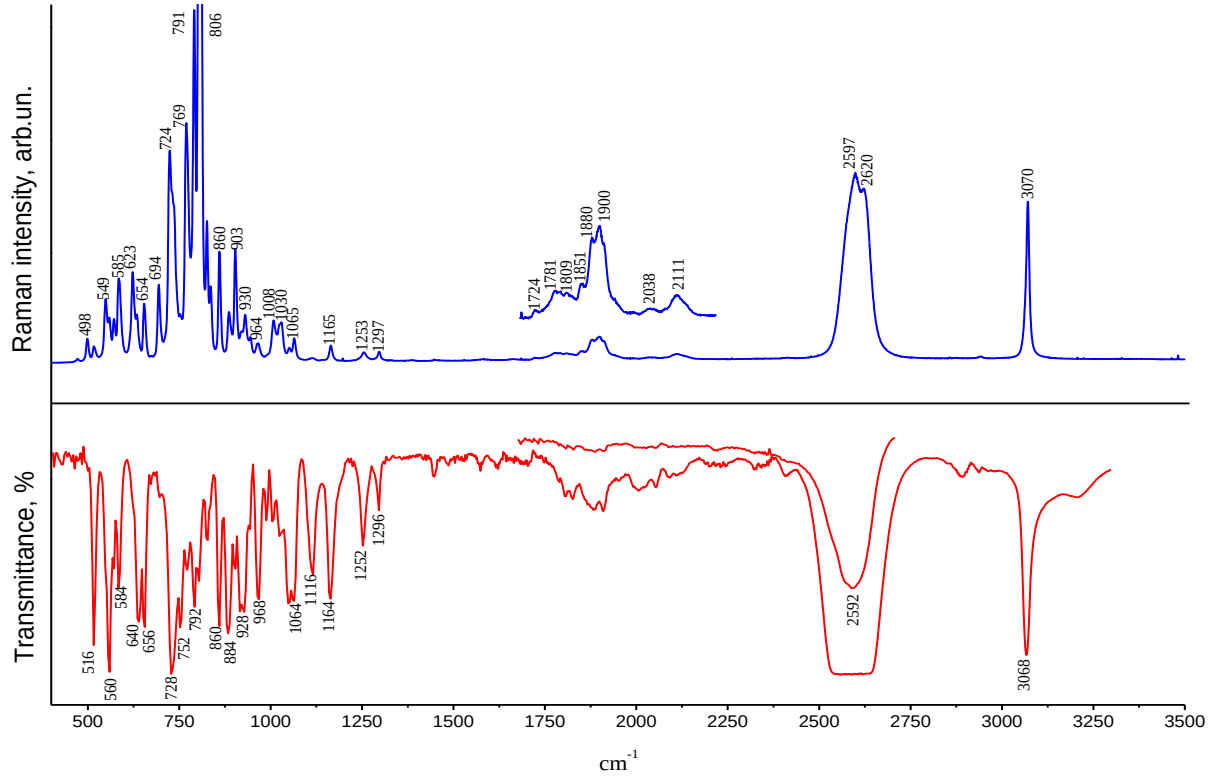

Figure. 2. Raman and IR spectra of solid 7,8,9-$C_3B_8H_{12}$ (**1**).

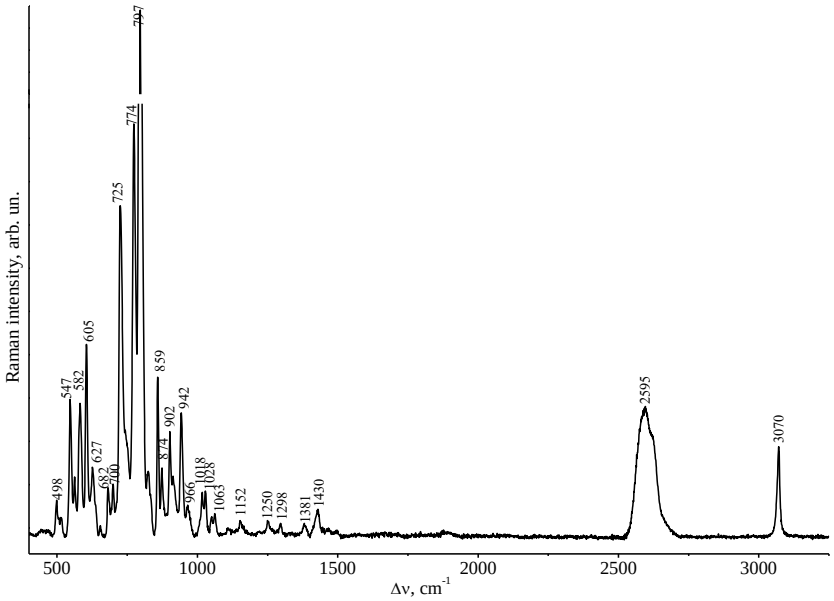

Figure 3. Raman spectrum of solid 7,8,9-$C_3B_8H_{11}D$ (μ-*d*-**1**).

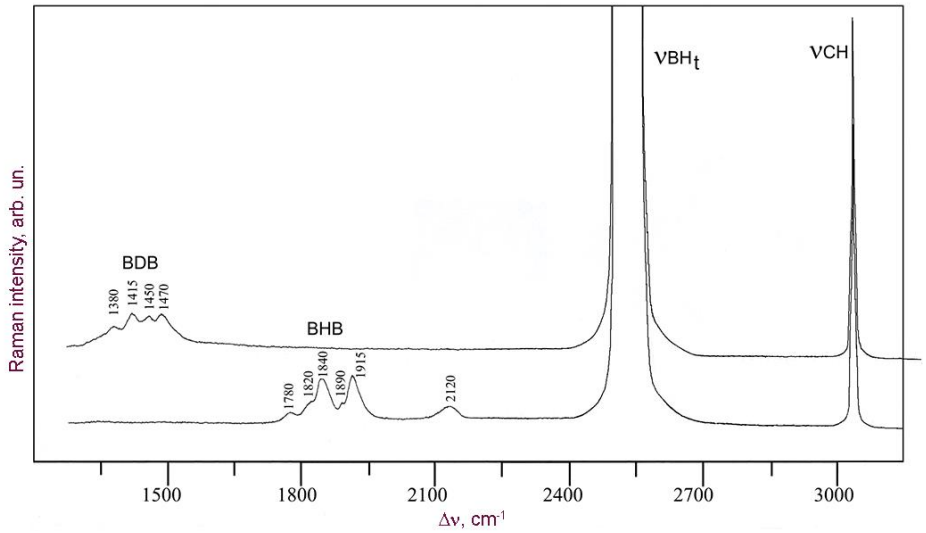

Figure 4. Detailed BHB and BDB Raman patterns for solid Cs[7,9-$C_2B_9H_{12}$] (**2**) and its μ-*d*-analog (μ-*d*-**2**) in comparison with their νBH_t and νCH regions.

that the calculation, as carried out in a harmonic approximation, correctly reproduces the frequencies in the middle region of the spectrum, but overvalues the frequencies in the region of 1800–3100 cm^{-1}. The only well-localized normal modes are those corresponding to the stretching vibrations with hydrogen atom participation, namely, ν/δ(BHB) (*vide infra*), νBH_t and νCH modes. The remaining normal modes are of heavily mixed origin.

The frequencies of analogous vibrations of **1** and **2** are compared in Table 1. In the νCH region, only one band is observed not only in the spectrum of **2**, in which two C–H bonds are separated, but also for **1** with its three adjacent C–H bonds (see Figs. 2–4 and Tables S1, S2 in ESI). The absence of kinematic interaction of adjacent νCH vibrational coordinates was observed previously for icosahedral *closo*-1,2-$C_2B_{10}H_{12}$ species [27] and was related to the specificity of C–C bonds in dicarbaborane cages [22b]. The frequency of the νCH mode for **1** (3070 cm^{-1}) is significantly higher than that for **2** (3030 cm^{-1})**.** The same is even truer for the νBH_t region (2597–2619 and 2520–2548 cm^{-1} for **1** and **2**, respectively). As is seen from Tables 1, S1, S2, all the rest salient features of the spectra of **1** and **2** nearly coincide. In particular, the most intense Raman lines corresponding to vibrations of the whole cage have similar frequencies (791, 806 cm^{-1} and 774, 797 cm^{-1}, respectively).

The vibrational modes including *extra*-hydrogen atom of 11-vertex *nido* polyhedra were analyzed in detail in Ref. [10]. The BHB moiety possesses three vibrational degrees of freedom. Normal coordinate analysis for **1** and **2** predicts two well-localized normal modes with frequencies in the regions ~1990 and ~1700 cm^{-1}. Animation of their eigenvectors demonstrates that the first one is a vertical displacement of the H_b atom (see Fig. 5 left). This is a symmetric stretch of both B–H_b bonds, but

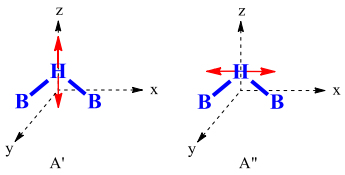

Figure 5. Vibrations of the BHB bridge.

it inevitably leads to a simultaneous change in the BHB angle; thus, we designate it as a ν/δ mode of A′ type. The second mode is the displacement of the H_b atom parallel to the B10–B11 line of the polyhedron open face (Fig. 5 right). This mode is an antisymmetric stretch of two B–H_b bonds and it also involves the angle deformation; thus, it is a ν/δ mode of A″ type. In the experimental spectra, these modes manifest themselves as weak features in the lengthy region of 1700–2150 cm^{-1} (Figs. 2, 4), which had been related to the *extra*-hydrogen vibrations still by Hawthorne *et al.* [23]. Note that the frequency region of BHB ν/δ modes is much lower than that of the terminal νB-H_t modes.

Deuteration of the *extra* hydrogen proves that all the spectral pattern in the region of 1700–2150 cm^{-1} originates from *extra*-hydrogen vibrations, because it disappears completely in the spectra of μ-deuterated species, being replaced by the corresponding ν(BDB) bands at ~1450 cm^{-1} and ~1380 cm^{-1} (with a normal H/D ratio of ~1.3). This is exemplified in Fig. 3 for **1** and in Fig. 4 for **2**. Special attention should be paid to an unusual shape of the νBHB pattern. It is complicated in both Raman and IR spectra, exhibiting a fine structure with many peaks, which remain in the spectra of solutions. A detailed discussion of this phenomenon on the example of methyldiborane spectra can be found in Ref. [28]. Analysis of the literature data allows one to conclude that this spectral pattern is explained by the extensive Fermi resonance, caused by interaction of the fundamental vibrational levels with overtone and/or combination levels of the same symmetry. With this in mind, small narrow peaks observed in this pattern in the spectra of **1** and **2** (Figs. 2, 4) can be interpreted as belonging to overtones or combinations of normal modes of mixed origin but with significant H_b atom participation, those situated in the region of 850–1150 cm^{-1}.

The results of NCA show that the third vibration with participation of the H_b atom is not localized. It is strongly coupled with other vibrational coordinates and takes part in several normal modes of A′ type. The frequencies of these mixed modes notably move to the lower values on μ-deuteration.

As is seen from Figs. 2, 3 and Tables 1, S1, S2, the spectra of carba-*nido*-undecaboranes studied exhibit no low-frequency modes, just like the *closo* carboranes [1]. The lowest-frequency modes in the spectra of **1** and **2** are those at 463 and 498 cm^{-1}, respectively. This means that the skeleton of both 11-vertex *nido* polyhedra explored, in spite of possessing "open faces", continues to be rigid, unlike that of 11-vertex *quasi-closo* congeners [11].

2. Molecular geometry and electron density distribution

According to the experimental and computed data on interatomic distances of isostructural species **1** and **2** (Table 2), the substitution of the boron atom at position 8 for the carbon one influences only the distances with participation of this atom, while the other distances remain unaffected. Notably, for both species **1** and **2**, the B10–B11 distance under the hydrogen bridge is elongated compared to other B–B distances in the *nido* cage, the fact which was observed for some polyhedral boranes [18] and is evidently due to a peculiarity of their bonding pattern.

The bonding systems in **1** and **2,** elucidated on the basis of topological analysis of the electron density (ED) function, appeared to have much in common. The connectivity in both molecules, like in other caged boranes and carbaboranes, is realized *via* both intracage two-center and multi-center bonds of reduced order and charge delocalization over their surfaces [20].

The results of AIM calculations are presented in Table 3. The corresponding molecular graphs are depicted in Fig. 6. The averaged value of electron density $\rho_b(\mathbf{r})$ in (3,–1) bond critical points (BCP) for terminal BH_t bonds in **1** is 0.187 a.u., which is higher than that for **2** (0.177 a.u.). A comparison of $\rho_b(\mathbf{r})$ magnitudes for the C–H bonds in **1** and **2** reveals the same tendency, *i.e.*, these are higher in **1** (0.3015 a.u.) than in **2** (0.294 a.u.). These differences are due to the influence of the third carbon atom in **1** and are reflected by an increase in vibrational frequencies of the corresponding bonds.

The values of ED $\rho_b(\mathbf{r})$ for BCPs of B–B and B–C two-center bonds lie in the interval of 0.115 ÷ 0.130 a.u. and 0.128 ÷ 0.147 a.u., respectively. It is worthy of note that the values of $\rho_b(\mathbf{r})$ for BH_b bonds of the BHB-bridges, equal for **1** and **2** (0.125 a.u.), are smaller than those for BH_t bonds. Remarkably, the values of $\rho_b(\mathbf{r})$ for BH_b bonds are comparable with those for intracage B–B bonds (Table 3). This means that the *extra*-hydrogen atom plays an essential role in the cage formation,

Table 2. Selected interatomic distances (**d**, Å) for **1** and **2**

Distance	**1** calc.[13]	**1** calc. CCSD	exp. for $(PSH)^+$ **2** [17]	exp.for Me_2S-**2** [16]	**2** calc. CCSD
av. C–H	1.086	1.080			1.084
av. B–H_t	1.188	1.178			1.191
B–H_b	1.312	1.307	1.23(3)	1.284 1.292	1.315
B10–B11	1.828	1.823	1.845	1.841	1.851
B10–C9 B11–C7	1.656	1.649	1.646 1.641		1.622
B2–C7 B5–C9	1.685	1.682			1.674
B6–B10 B6–B11	1.797	1.794			1.807
B3–C7 B4–C9	1.698	1.696			1.698
B2–B11 B5–B10	1.803	1.797			1.822
B3–B4	1.767	1.765			1.751
B2–B6 B5–B6	1.778	1.796			1.796
B2–B3 B4–B5	1.755	1.754			1.765
B1–B6	1.800	1.796			1.799
B1–B3 B1–B4	1.775	1.770			1.797
B1–B2 B1–B5	1.759	1.755			1.755
B3–B8 B4–B8		1.728			1.810

Table 3. QTAIM topological parameters for **1** and **2** calculated at CCSD/cc-pVTZ level

Dist.	1			2		
	ρ(r), a.u.	**$\nabla^2\rho$(r), a.u.**	**H_e, a.u.**	**ρ(r), a.u.**	**$\nabla^2\rho$(r), a.u.**	**H_e, a.u.**
av. C–H	0.30153	–1.26514	–0.3547	0.29378	–1.19879	–0.3487
av. B–H_t	0.18670	–0.20121	–0.2076	0.17714	–0.12014	–0.1906
B–H_b	0.12530	0.16106	–0.1064	0.12475	0.17654	–0.1053
B10–B11	–	–	–			
B10–C9 B11–C7	0.14400	0.08220	–0.1346	0.14677	0.02511	–0.1401
B2–C7 B5–C9	0.12841	0.09683	–0.1133	0.13564	0.09054	–0.1230
B3–C7 B4–C9	0.12777	–0.02013	–0.1137	0.12906	0.12395	–0.1135
B6–B10 B6–B11	0.12453	–0.18716	–0.0798	0.12535	–0.19468	–0.0812
B2–B11 B5–B10	–	–	–			
B3–B4	0.12445	–0.16409	–0.0818	0.13633	–0.23862	–0.0948
B2–B6 B5–B6	0.12522	–0.18387	–0.0847	0.12417	–0.17522	–0.0801
B2–B3 B4–B5	–	–	–			
B1–B6	0.11982	–0.15049	–0.0753	0.12232	–0.16089	–0.0778
B1–B3 B1–B4	0.12728	–0.18297	–0.0928	0.12448	–0.16567	–0.0778
B1–B2 B1–B5	0.12823	–0.19064	–0.0904	0.13005	–0.19935	–0.0910
B3–B8 B4–B8	0.12438	–0.15781	–0.0870	0.11455	–0.11583	–0.0881

comparable to that of boron atoms. H_b atom completes the cage bonding system to 2(n+2) electrons, in accord with the Williams–Wade skeletal electron counting rules [29, 30].

The values of the Laplacian of electron density ($\nabla^2\rho_b$) of B–H_b bonds are 0.161 a.u. and 0.176 a.u. for **1** and **2**, respectively; their signs are positive. These data along with the relatively high value of ρ_b(**r**) mean that boron–hydrogen interaction in the bridges is of intermediate type, according to Bader, the BCPs of these bonds are shifted towards boron atoms. The same is true of B–C bonds. It is also notable that the values of local energy density (H_e) are all negative [31]. This means that all the above-mentioned bonds are covalent but polar.

Species **1** and **2** exhibit an interesting feature, found previously for some other representatives of polyhedral boranes and carbaboranes [20, 32], namely, the absence of BCP's for some pairs of adjacent boron atoms. This means that not all the edges of the polyhedron depicted in Fig. 1 correspond to two-center bond paths. In particular, in both compounds studied, B10 and B11 atoms involved in the BHB bridge are not linked by the lines of a maximum charge density, and here is the reason of elongation of the corresponding interatomic distances (Table 2). The fact of the absence of BCP between boron atoms participating in the BHB bridge was first reported by Bader and Legar for *nido*-borane B_5H_9 [20]. We have obtained analogous results also for 11-vertex *nido*-carbaboranes $[CB_{10}H_{13}]^-$ and 11-Me-2,7-$C_2B_9H_{12}$ [10]. It is obvious that this phenomenon is a consequence of the *extra*-hydrogen influence on the electronic structure of the species investigated. However, the lack of the B10–B11 bond path does not mean that there is no interaction between these atoms. Three-centered delocalization index [33, 34] calculated for the group of three atoms B10H_bB11 has the value of 0.099 a.u. for **1** and 0.103 a.u. for **2**, which means, with an allowance for the data of Ref. [11], that these atoms interact *via* an open three-center bond.

Due to the absence of edge-localized B10–B11 bond paths, the "open faces" of both molecules are in fact not pentagonal, as it is commonly accepted, since they involve not only C and B atoms, but also H_b atoms. Thus, six-membered rings are formed, encompassing (C7C8C9B10H_bB11) (**1**) and (C7B8C9B10H_bB11) (**2**) atoms (Fig. 6). These rings are characterized by (3,+1) ring critical points (RCP) with low ρ_r(**r**) values (0.028 a.u.), much lower than ρ_r(**r**) for the smaller rings (0.100–0.120 a.u.).

Moreover, in **1** and **2** some other pairs of boron atoms are not connected by bond paths, though their interatomic distances, being slightly elongated (Table 2), are still in the limit of "normal" B–B distances. These are B2–B11 = B5–B10 and B2–B3 = B4–B5 pairs (Fig. 6). It is also important that the values of ρ_r(**r**) in RCP for three- and four-membered rings do not differ significantly from the values of ρ_b(**r**) for C–B and B–B bonds. The latter is typical for polyhedral boron species and points to substantial charge delocalization over the cage surface.

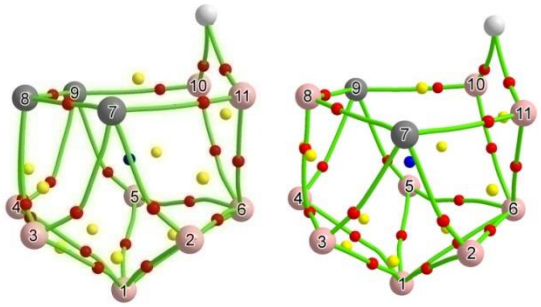

Figure 6. Molecular graphs of molecule 7,8,9-$C_3B_8H_{12}$ (**1**) (left) and isolated anion $[7,9\text{-}C_2B_9H_{12}]^-$ (**2**) (right) obtained as a result of the topological analysis of the electron density distribution function. The bond and ring critical points are denoted by small red and yellow circles, respectively.

It is pertinent to mention here that when the *extra*-hydrogen atom is removed from the open face of the 11-vertex *nido*-polyhedron with formation of tri- or dicarbollide ions, all the edges of the open face do correspond to localized two-center bonds in their molecular graphs. This is also evident from a shortening of the corresponding interatomic distance. For example, in the X-ray structures of various salts of 7,8,9-tricarbollide anion, the B10–B11 distance is only 1.725 Å [35b], or 1.719 Å [35c], or 1.733 Å [14] compared to ~1.8 Å in **1**.

Experiment and calculations

1. Synthesis

$C_3B_8H_{12}$ (1) and $C_3B_8H_{11}D$ (μ-d-1)

Tricarbaborane $C_3B_8H_{12}$ and its μ-deuterated derivative $C_3B_8H_{11}D$ were obtained using a slightly modified literature

procedure [12]. Salt $[Me_4N]C_3B_8H_{11}$ (104 mg, 0.4 mmol) was dissolved in CF_3COOH or CF_3COOD (4 mL). The resulting solution was covered with hexane (10 mL) and stirred for 3 h under protective argon atmosphere. Then the hexane layer was transferred to a sublimation apparatus and evaporated to dryness at room temperature. A further sublimation of the oily residue at *ca*. 100 °C/0.1 mm Hg gave $C_3B_8H_{12}$ or $C_3B_8H_{11}D$, respectively (44 mg, 82% yield). The $^{11}B\{^1H\}$ NMR spectra of both compounds were almost identical. $^{11}B\{^1H\}$ NMR (400 MHz, $CDCl_3$): δ = 0.5 (2 B), –19.0 (2 B), –19.9 (2 B), –26.0 (1 B), –35.2 (1 B).

Cs[7,9-$C_2B_9H_{12}$] and Cs[7,9-$C_2B_9H_{11}D$] were obtained by the method described previously [15] and kindly delivered by V. N. Kalinin.

2. Vibrational spectra

Raman spectra for the solid samples sealed in capillaries and also for a saturated aqueous solution of salt **2** were recorded in the region of 100–3500 cm^{-1} using LabRAM and U-1000 Jobin-Yvon laser Raman spectrometers. The spectra were excited with the 632.8 nm line of a He–Ne laser and the 514.5 nm line of an Ar^+ laser (Spectra Physics 2020). Depolarization ratios of the Raman lines in the spectrum of the aqueous solution of **2** were estimated qualitatively. The IR spectra in the region of 150–3500 cm^{-1} for solids **1** and **2** pressed with polyethylene and for their Nujol mulls and KBr pellets were obtained using an M-82 Carl Zeiss spectrophotometer and a Nicolet Magna-750 FTIR spectrometer.

3. Computation details

Geometry optimization and normal coordinate analysis as well as calculations of IR intensities were carried out at B3LYP/6-311++G(d,p) level using the G09 program suite [36]. Topological analysis of the theoretical electron density distribution (based on the results of the DFT calculation) was accomplished at CCSD/cc-pVTZ level using the AIMAll program [37].

Conclusions

1. The BH_b bonds in the BHB bridge of two isostructural *nido* species, molecule 7,8,9-$C_3B_8H_{12}$ (**1**) and anion 7,9-$[C_2B_9H_{12}]^-$ (**2**), are sufficiently sound chemical bonds, to which CPs of (3,–1) type with the high values of electron density correspond. The latter values are comparable with those for intracage B–B bonds, thus demonstrating that the bridging H_b atom is an equal partner in formation of the cage bonding system. QTAIM data show that there is no edge-localized bond path between B10 and B11 atoms, here is a rationale for this distance elongation compared to other interboron distances.

2. Vibrations of the bridge H_b atom in species **1** and **2** give rise to two well-localized normal modes predicted at ~1700 and ~1990 cm^{-1}, those of A″ and A′ symmetry species. The complicated spectral pattern with a fine structure observed in this region (1700–2150 cm^{-1}) is due to the extensive Fermi resonance.

3. An increase in the number of carbon atoms in the polyhedron open face from two to three leads to strengthening of the C–H and terminal B–H bonds, while those within the cage and in the BH_bB bridge stay unaffected.

Acknowledgements

This work was supported by the Ministry of Science and Higher Education of the Russian Federation.

The authors are indebted to V. N. Kalinin for the synthesis of salt Cs[7,9-$C_2B_9H_{12}$] and its μ-deuterated species.

Corresponding author

* E-mail: buklei@ineos.ac.ru. Tel: +7(499)135-9262 (L. A. Leites)

Electronic supplementary information

Electronic supplementary information (ESI) available online: Raman and IR spectra of **2**; assignment of vibrational spectra for **1**, μ-*d*-**1**, **2** and μ-*d*-**2**. For ESI, see DOI: 10.32931/io1915a

References

1. L. A. Leites, *Chem. Rev*., **1992**, *92*, 279–323. DOI: 10.1021/cr00010a006
2. D. Seyferth, K. D. Buchner, W. S. Rees Jr., L. Wesemann, W. M. Davis, S. S. Bukalov, L. A. Leites, H. Bock, B. Solouki, *J. Am. Chem. Soc*., **1993**, *115*, 3586–3594. DOI: 10.1021/ja00062a023
3. A. Salam, M. S. Deleuze, J.-P. François, *Chem. Phys*., **2001**, *271*, 17–30. DOI: 10.1016/S0301-0104(01)00420-7
4. A. Salam, M. S. Deleuze, J.-P. François, *Chem. Phys*., **2003**, *286*, 45–61. DOI: 10.1016/S0301-0104(02)00907-2
5. E. G. Kononova, S. S. Bukalov, L. A. Leites, K. A. Lyssenko, V. A. Ol'shevskaya, *Russ. Chem. Bull*., **2003**, *52*, 85–92. DOI: 10.1023/A:1022436029305
6. E. G. Kononova, L. A. Leites, S. S. Bukalov, A. V. Zabula, I. V. Pisareva, V. E. Konoplev, I. T. Chizhevsky, *Chem. Phys. Lett.*, **2004**, *390*, 279–284. DOI: 10.1016/j.cplett.2004.04.025
7. E. G. Kononova, L. A. Leites, S. S. Bukalov, A. V. Zabula, I. V. Pisareva, V. E. Konoplev, I. T. Chizhevsky, *Russ. Chem. Bull*., **2004**, *53*, 944–945. DOI: 10.1023/B:RUCB.0000037870.23093.e7
8. E. G. Kononova, L. A. Leites, S. S. Bukalov, I. V. Pisareva, I. T. Chizhevsky, *J. Mol. Struct.*, **2006**, *794*, 148–153. DOI: 10.1016/j.molstruc.2006.01.051
9. E. G. Kononova, L. A. Leites, S. S. Bukalov, I. V. Pisareva, I. T. Chizhevsky, J. D. Kennedy, J. Bould, *Eur. J. Inorg. Chem*., **2007**, 4911–4918. DOI: 10.1002/ejic.200700461
10. L. A. Leites, E. G. Kononova, S. S. Bukalov, *Collect. Czech. Chem. Commun.*, **2007**, *72*, 1659–1675. DOI: 10.1135/cccc20071659
11. L. A. Leites, R. R. Aysin, E. G. Kononova, S. S. Bukalov, *Russ. Chem. Bull*., **2018**, *67*, 1340–1349. DOI: 10.1007/s11172-018-2223-3
12. B. Štíbr, J. Holub, F. Teixidor, C. Viñas, *J. Chem. Soc., Chem. Commun*., **1995**, 795–796. DOI: 10.1039/C39950000795
13. J. Holub, B. Štíbr, D. Hnyk, J. Fusek, I. Cisařová, F. Teixidor, C. Viñas, Z. Plzák, P. v. R. Schleyer, *J. Am. Chem. Soc*., **1997**, *119*, 7750–7759. DOI: 10.1021/ja971194u
14. M. Bakardjiev, J. Holub, D. Hnyk, I. Ćisařová, M. G. S. Londesborough, D. S. Perekalin, B. Štíbr, *Angew. Chem., Int. Ed*., **2005**, *44*, 6222–6226. DOI: 10.1002/anie.200501018

15. M. F. Hawthorne, D. C. Young, P. M. Garrett, D. A. Owen, S. G. Schwerin, F. N. Tebbe, P. A. Wegner, *J. Am. Chem. Soc*., **1968**, *90*, 862–868. DOI: 10.1021/ja01006a006
16. V. Subrtova, C. Novak, A. Linek, J. Hasek, *Acta Crystallogr*., *Sect. C*: *Cryst. Struct. Commun.*, **1984**, *40*, 1955–1956. DOI: 10.1107/S0108270184010209
17. M. A. Fox, A. E. Goeta, A. K. Hughes, A. L. Johnson, *J. Chem. Soc.*, *Dalton Trans*., **2002**, 2132–2141. DOI: 10.1039/B108937D
18. (a) M. A. Fox, A. K. Hughes, J. M. Malget, *J. Chem. Soc*., *Dalton Trans*., **2002**, 3505–3517. DOI: 10.1039/B203920F; (b) G. F. Mitchell, A. J. Welch, *J. Chem. Soc.*, *Dalton Trans*., **1987**, 1017–1025. DOI: 10.1039/DT9870001017
19. R. F. W. Bader, *Atoms in Molecules: a Quantum Theory*, Clarendon Press, Oxford, UK, **1990**.
20. (a) R. F. W. Bader, D. A. Legare, *Can. J. Chem*., **1992**, *70*, 657–676. DOI: 10.1139/v92-089; (b) T. A. Keith, R. F. W. Bader, Y. Aray, *Int. J. Quant. Chem*., **1996**, *57*, 183–198. DOI: 10.1002/(SICI)1097-461X(1996)57:2<183::AID-QUA4>3.0.CO;2-U
21. (a) M. Yu. Antipin, A. V. Polyakov, V. G. Tsirel'son, M. Kappkhan, V. V. Grushin, Yu. T. Struchkov, *Organomet. Chem. (USSR)*, **1990**, *3*, 421; (b) M. Antipin, R. Boese, D. Bläser, A. Maulitz, *J. Am. Chem. Soc*., **1997**, *119*, 326–333. DOI: 10.1021/ja961884i; (c) K. A. Lyssenko, M. Yu. Antipin, V. N. Lebedev, *Inorg. Chem*., **1998**, *37*, 5834–5843. DOI: 10.1021/ic9807644
22. (a) K. A. Lyssenko, D. G. Golovanov, V. I. Mesheryakov, A. R. Kudinov, M. Yu. Antipin, *Russ. Chem. Bull*., **2005**, *54*, 933–941. DOI: 10.1007/s11172-005-0337-x; (b) I. V. Glukhov, K. A. Lyssenko, A. A. Korlyukov, M. Yu. Antipin, *Russ. Chem. Bull*., **2005**, *54*, 547–559. DOI: 10.1007/s11172-005-0289-1
23. D. V. Howe, C. J. Jones, R. J. Wiersema, M. F. Hawthorne, *Inorg. Chem*., **1971**, *10*, 2516–2523. DOI: 10.1021/ic50105a029
24. L. A. Leites, S. S. Bukalov, L. E. Vinogradova, V. N. Kalinin, N. I. Kobel'kova, L. I. Zakharkin, *Bull. Acad. Sci. USSR, Div. Chem. Sci.*, **1984**, *33*, 880. DOI: 10.1007/BF00947866
25. L. A. Leites, Dr. Sci. Thesis, INEOS RAS, Moscow, **1986**.
26. (a) S. S. Bukalov, L. A. Leites, *Izv. Akad. Nauk SSSR, Ser. Fiz*., **1989**, *53*, 1715; (b) S. S. Bukalov, L. A. Leites, A. L. Blumenfeld, E. I. Fedin, *J. Raman Spectr*., **1983**, *14*, 210–211. DOI: 10.1002/jrs.1250140315
27. L. A. Leites, S. S. Bukalov, *Bull. Acad. Sci. USSR, Div. Chem. Sci.*, **1989**, *38*, 2079–2082. DOI: 10.1007/BF00962111
28. (a) J. H. Carpenter, W. J. Jones, R. W. Jotham, L. H. Long, *Spectrochim. Acta, Part A*, **1970**, *26*, 1199–1214. DOI: 10.1016/0584-8539(70)80027-7; (b) J. H. Carpenter, W. J. Jones, R. W. Jotham, L. H. Long, *Spectrochim. Acta, Part A*, **1971**, *27*, 1721–1734. DOI: 10.1016/0584-8539(71)80227-1; (c) R. W. Jotham, J. S. McAvoy, D. J. Reynolds, *J. Chem. Soc., Dalton Trans.*, **1972**, 473–479. DOI: 10.1039/DT9720000473
29. (a) R E. Williams, *Inorg. Chem.*, **1971**, *1*, 210–214. DOI: 10.1021/ic50095a046; (b) R. E. Williams, *Adv. Inorg. Chem. Radiochem.*, **1976**, *18*, 67–142. DOI: 10.1016/S0065-2792(08)60028-X; (c) R. E. Williams, *Chem. Rev*., **1992**, *92*, 177–207. DOI: 10.1021/cr00010a001; (d) R. E. Williams, J. W. Bausch, in: *Boron Chemistry at the Beginning of the 21st Century*, Yu. N. Bubnov (Ed.), Editorial URSS, Moscow, **2003**, pp. 3–16.
30. (a) K. Wade, *Adv. Inorg. Chem. Radiochem.*, **1976**, *18*, 1–66. DOI: 10.1016/S0065-2792(08)60027-8; (b) M. A. Fox, K. Wade, in: *Boron Chemistry at the Beginning of the 21st Century*, Yu. N. Bubnov (Ed.), Editorial URSS, Moscow, **2003**, pp. 17–26.
31. D. Cremer, E. Kraka, *Angew. Chem., Int. Ed.*, **1984**, *23*, 627–628. DOI: 10.1002/anie.198406271
32. K. A. Lyssenko, Ph. D. Thesis, INEOS RAS, Moscow, **2001**.
33. J. Poater, M. Duran, M. Solà, B. Silvi, *Chem. Rev*., **2005**, *105*, 3911–3947. DOI: 10.1021/cr030085x
34. R. Bochicchio, R. Ponec, A. Torre, L. Lain, *Theor. Chem. Acc*., **2001**, *105*, 292–298. DOI: 10.1007/s002140000236
35. (a) B. Štíbr, J. Holub, I. Ćisařová, F. Teixidor, C. Viñas, *Inorg. Chim. Acta*, **1996**, *245*, 129–131. DOI: 10.1016/0020-1693(96)05082-7; (b) B. Štíbr, J. Holub, I. Císařová, F. Teixidor, C. Viñas, J. Fusek, Z. Plzák, *Inorg. Chem.*, **1996**, *35*, 3635–3642. DOI: 10.1021/ic951437o; (c) J. Holub, A. Růžička, Z. Padělková, B. Štíbr, *J. Organomet. Chem.*, **2011**, *696*, 2742–2745. DOI: 10.1016/j.jorganchem.2011.04.021
36. Gaussian 09, Revision D.01, M. J. Frisch, G. W. Trucks, H. B. Schlegel, G. E. Scuseria, M. A. Robb, J. R. Cheeseman, G. Scalmani, V. Barone, B. Mennucci, G. A. Petersson, H. Nakatsuji, M. Caricato, X. Li, H. P. Hratchian, A. F. Izmaylov, J. Bloino, G. Zheng, J. L. Sonnenberg, M. Hada, M. Ehara, K. Toyota, R. Fukuda, J. Hasegawa, M. Ishida, T. Nakajima, Y. Honda, O. Kitao, H. Nakai, T. Vreven, J. A. Montgomery, Jr., J. E. Peralta, F. Ogliaro, M. Bearpark, J. J. Heyd, E. Brothers, K. N. Kudin, V. N. Staroverov, T. Keith, R. Kobayashi, J. Normand, K. Raghavachari, A. Rendell, J. C. Burant, S. S. Iyengar, J. Tomasi, M. Cossi, N. Rega, J. M. Millam, M. Klene, J. E. Knox, J. B. Cross, V. Bakken, C. Adamo, J. Jaramillo, R. Gomperts, R. E. Stratmann, O. Yazyev, A. J. Austin, R. Cammi, C. Pomelli, J. W. Ochterski, R. L. Martin, K. Morokuma, V. G. Zakrzewski, G. A. Voth, P. Salvador, J. J. Dannenberg, S. Dapprich, A. D. Daniels, O. Farkas, J. B. Foresman, J. V. Ortiz, J. Cioslowski, and D. J. Fox, Gaussian, Inc., Wallingford CT, **2013**.
37. AIMAll (Version 17.11.14), T. A. Keith, TK Gristmill Software, Overland Park KS, USA, **2017** (aim.tkgristmill.com).